Preprint
UCRL-JC-142523

Second Order Optical Nonlinearities in Thermally Poled Phosphate Glasses

P. Thamboon, D. Krol

This article was submitted to The Society of Photo-Optical Instrumentation Engineers Proceedings (SPIE)
Photonics West, San Jose, CA., January 19-25, 2002

January, 2002

U.S. Department of Energy

Lawrence Livermore National Laboratory

Second order optical nonlinearities in thermally poled phosphate glasses

Prissana Thamboon and Denise M. Krol
Dept. of Applied Science, Univ. of California at Davis
Lawrence Livermore National Laboratory

ABSTRACT

Second order optical nonlinearities were induced in commercial phosphate glasses (Schott, IOG-1) by the thermal poling technique. The induced $\chi^{(2)}$ was measured via second harmonic generation using a fundamental beam from a 1064 nm mode-locked Nd:YAG laser. The nonlinear regions were characterized using the Maker-Fringe technique, in which the second harmonic signals were observed as a function of incident angle of the fundamental beam. The results show that the $\chi^{(2)}$ profile has contributions from two distinct regions: a near-anodic surface region and a bulk. We have modeled the induced profile to fit our experimental results. The dependence of the induced nonlinearity on applied poling fields, temperatures and poling time is discussed.
Keywords: thermal poling, frequency doubling, phosphate glasses

1. INTRODUCTION

The integration of all-optical devices onto one single substrate is becoming an area of intense research. Glasses are suitable substrates due to their good optical quality, low loss and flexible choice of compositions. An example of such a device is the integrated frequency-doubled waveguide laser shown in Fig. 1. In this device a glass waveguide in a rare-earth doped glass substrate is combined with Bragg gratings, serving as cavity mirrors, and a $\chi^{(2)}$ grating to double the frequency of the fundamental beam. We have chosen phosphate glasses as our host material because they can incorporate large concentration of rare earth ions to work as a laser or an amplifier. In particular, IOG-1, a phosphate glass developed by Schott Glass Technologies for integrated optics applications, is a suitable substrate material, since waveguides can be fabricated in it using the ion-exchange technique[1-3]. Bragg gratings can be implemented by the UV writing technique. A segment with a second-order optical nonlinearity ($\chi^{(2)}$), necessary for frequency doubling and electro-optic modulation, is desired in order to fully exploit the potential use of phosphate glass-based optical waveguide devices. However, due to their inversion symmetry, glasses do not exhibit second order optical nonlinear effects. Nevertheless, Myers *et al.*[4] found that a thin layer of $\chi^{(2)}$ could be induced in fused silica by electric field poling (3-5 kV) at elevated temperatures (250-325 °C), the so-called thermal poling technique. Since then it has been shown that thermal poling can be used to induce a $\chi^{(2)}$ in a wide variety of glass compositions[4-7], but so far no poling studies have been reported for IOG-1. Here we present the results of our poling experiments on phosphate glasses. We find that a $\chi^{(2)}$ can be induced in IOG-1 glasses. We report on its dependence on poling field, poling temperature and poling time and describe procedures to obtain the nonlinear profile.

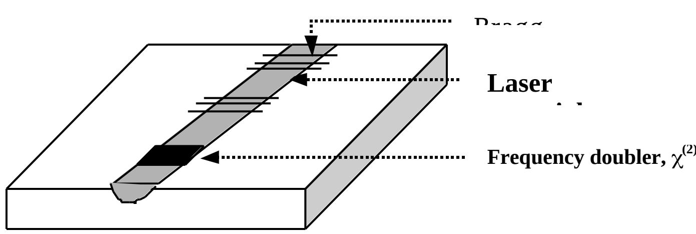

Fig. 1: Schematic of integrated waveguide device.

2. EXPERIMENTAL

2.1 Thermal poling

Commercial phosphate glasses, IOG-1, from Schott Glass Technologies, Inc., were used in our thermal poling experiments. These glasses, specially designed for integrated waveguide devices, have compositions in mole percent as follows: 60%P_2O_5, 24%Na_2O, 13%Al_2O_3, 3%R_2O_3, where R is Ce^{3+}. The 1 mm-thick samples were coated with Al in an evaporator. The Al-coated samples were placed in between stainless steel electrodes inside an oven. DC fields were applied across the samples while heating the samples to certain poling temperatures for certain poling times. Poling temperatures ranging from 100 to 250 ° C and poling times ranging from 20 to 60 minutes were investigated. Once the samples were cooled down to room temperature, the bias fields were removed. Then the Al coating was removed by etching the samples in diluted HCL solution before second harmonic generation (SHG) measurements.

2.2 Characterization of the nonlinear region

The induced SH signals were measured using a 1064 nm mode-locked Nd: YAG laser (100 ps pulse width, 76 MHz repetition rate, 20 W average power) as a fundamental beam. The induced nonlinear regions can be deduced via the Maker fringe technique[8] by observing the oscillation of the SH signals as a function of incident angle. The detailed set up is shown in Figure 2. The fundamental beam was focused through a 10-cm focal length lens into the poled sample, which was placed on a motorized rotational stage. A half-wave plate selected an appropriate polarization for the fundamental beam. The SH signals from the sample were separated from the fundamental beam using a harmonic beamsplitter and were sent through a short pass filter and a narrow bandwidth 532 nm pass filter to a photomultiplier tube. A LabView program controlled the rotation stage and obtained the SH signals from a lock-in amplifier.

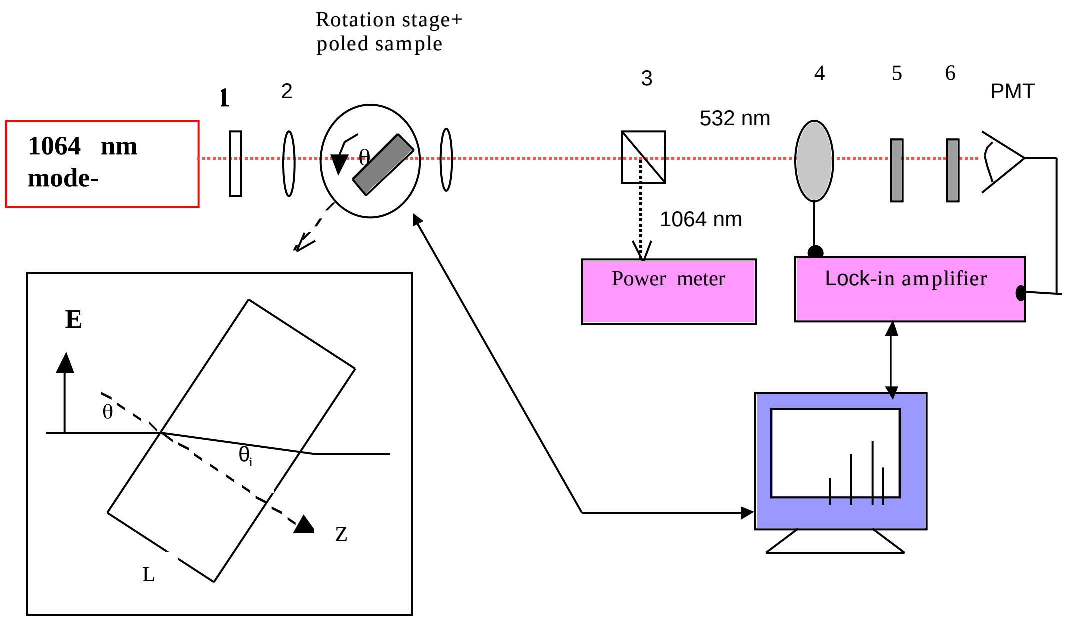

Fig. 2: Experimental set-up for measuring Maker fringe patterns in poled glasses. 1: Half-wave plate; 2: Lenses; 3: Harmonic beamsplitter; 4: Chopper; 5: Short pass filter; 6: 532 nm pass filter. The inset shows larger details in Maker fringe configuration.

3. RESULTS

Fig. 3 shows the Maker fringe pattern of an IOG-1 sample, poled at 1 kV and 150 °C for 40 minutes. The signal at room temperature does not decay with time at present as indicated in the two consecutive measurements (run B is 4 months after run A). The fringe pattern shows a rapid oscillation over a slow modulation. It should be pointed out that similar kind of fringe pattern has been observed for other poled glasses[9-13]. The maximum SH signal, is about 10^{-6} of that α-quartz for the same intensity of the fundamental beam. For the α-quartz measurement, the sample orientation is (010)[14].

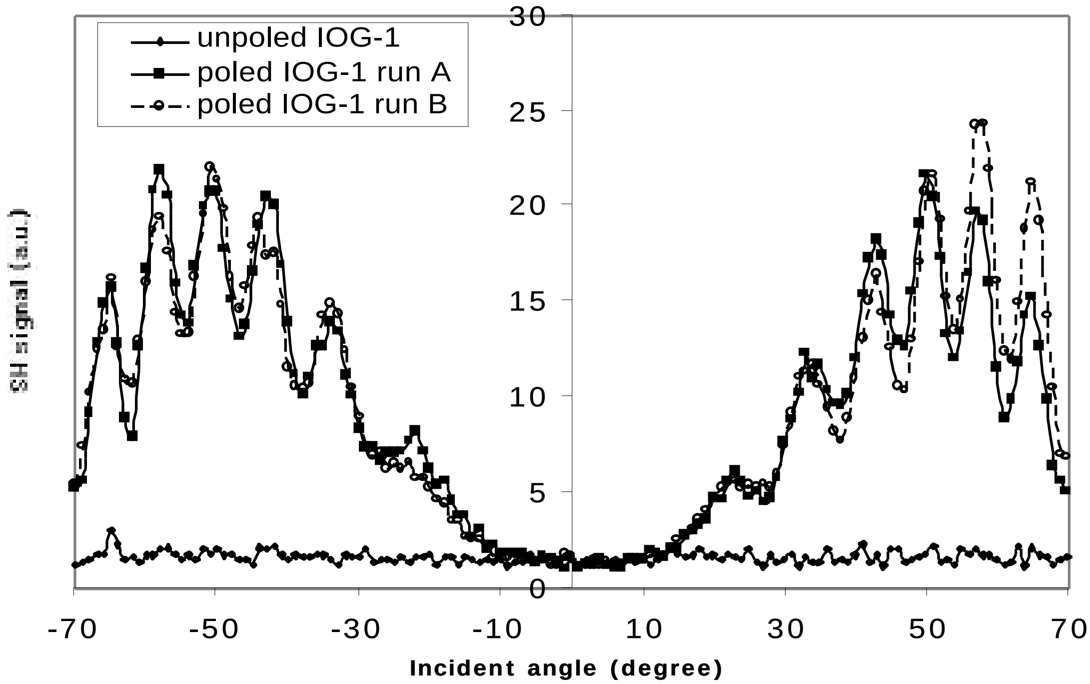

Fig. 3: Maker fringe patterns of a poled IOG-1 sample compared to an unpoled one. The poling condition is 1 kV, 150 ° C and 40 minutes poling time. Run A was measured after poling and run B was measured 4 months after run A.

We also investigated the effect of poling temperature and time on the induced SH signal. Table 1 summarizes the results for samples poled at 1 kV. The rapid oscillation feature is present at any poling temperature and time while the slow modulation feature appears and becomes more dominant at higher temperatures and longer poling times. The overall SH signals, shown in Table 1 in arbitrary units relative to the result at 150 C and 40 minutes, increase as poling temperature and time increase.

Table 1: Maker fringe characteristics at a 1kV poling voltage as poling temperatures and times were varied.

Time (min.) / Temp (°C)	**20**	**40**	**60**
100	N/A	Rapid	N/A
150	Rapid	Rapid + Slow SH signal ≈ 1	Rapid + Slow SH signal ≈ 1.4
200	Rapid + Slow SH signal ≈ 1.8	Rapid + Slow SH signal ≈ 2.1	Rapid + Slow SH signal ≈ 3
250	N/A	Rapid + Slow SH signal ≈ 3.3	N/A

The dependence on applied field at fixed temperatures and poling times is shown in Fig. 4. With a higher applied voltage, the slow modulation increases relative to the rapid oscillation feature as can be seen when comparing the adjusted signals of 1kV (multiplied by 4) to the signal of 2 kV applied voltages. An overshoot current observed at a higher voltage during the poling process limits experiments at higher applied voltages. This is due to a high concentration of mobile Na^+ ions in IOG-1 samples.

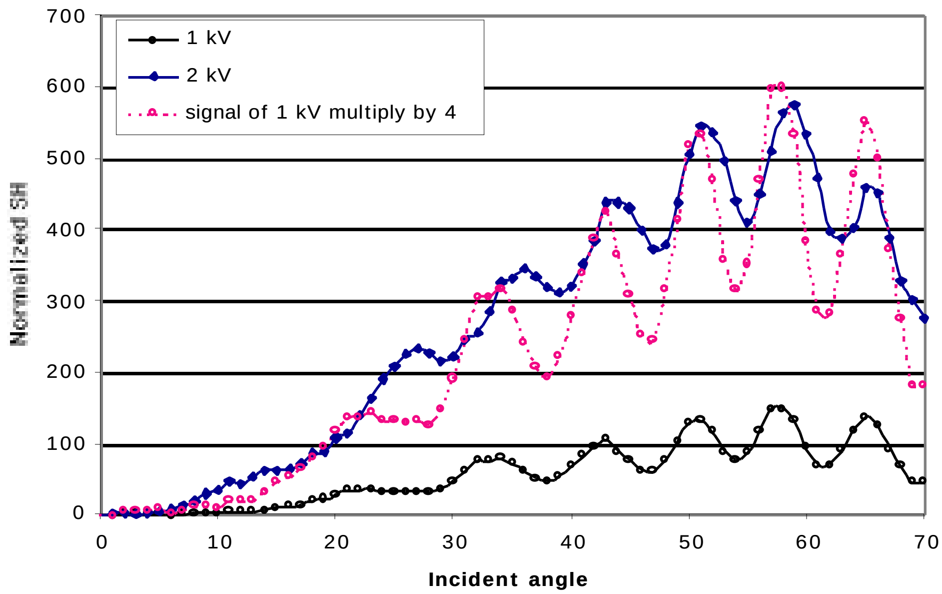

Fig. 4: Maker fringe patterns of an IOG-1 sample poled at 150 ° C for 40 minutes with different poling voltages.

In order to determine the thermal stability of the induced $\chi^{(2)}$, poled samples were subjected to heat treatment in the absence of the applied field. Typical results are shown in Fig. 5 for samples poled with 1 kV applied field, at 150 °C for 40 minutes. A significant drop in signal is observed for treatment temperatures above 200 °C. The slow modulation feature disappeared at 400 °C, whereas the rapid oscillation feature, although reduced in magnitude, still remained.

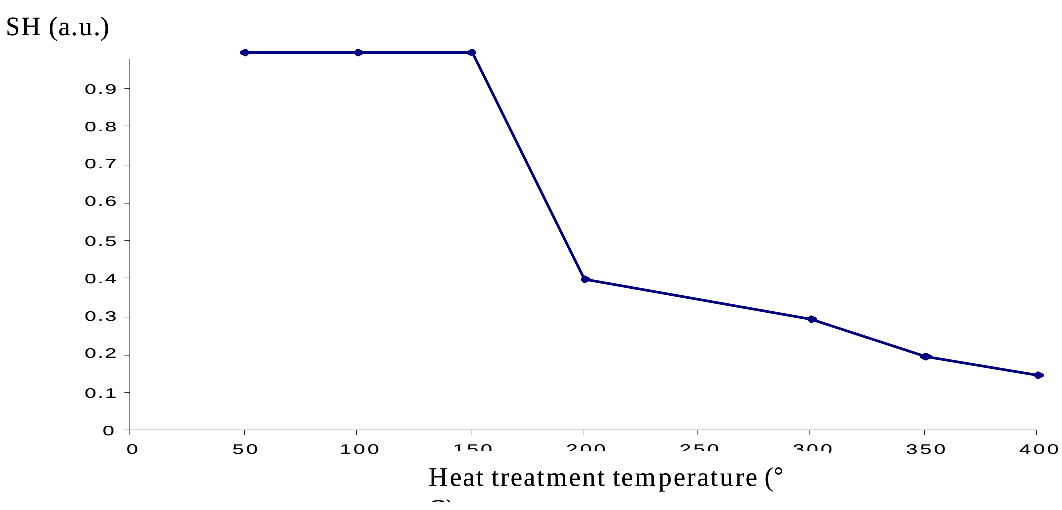

Fig. 5: The effect of heat treatment on the SH signals of samples poled at 1kV, 150 C for 40 minutes.

4. DISCUSSIONS

The Maker fringe patterns that we observe for poled IOG-1 samples contain information about the spatial profile of the induced second-order nonlinearity. In general[15], the SH signal depends on the nonlinear coefficient and the length of the nonlinear region as shown in expression (1)

$$I_{2\omega} \quad (I_\omega \, d \sin(\pi l/2l_c))^2 \qquad (1)$$

where $I_{2\omega}$ and I_ω are SH and fundamental intensity respectively, d is equal to $\chi^{(2)}/2$, l is sample length along propagation direction, l_c is a coherence length of the interaction between the SH and fundamental beam and is equal to $4\pi(n_{2\omega}-n_\omega)/\lambda_\omega$. In the Maker fringe experiment, rotation of the sample effectively varies the length along propagation direction. The nonlinear profile can in principle be derived from the fringe magnitude and its oscillation pattern.

For p- polarization , as shown in the inset of Fig. 2, and assuming $d_{33}= 3d_{31}$, since poled glasses belong to $C_{\infty v}$ point group symmetry, equation (1) can be written as

$$I_{2\omega} \quad \left\{ I_\omega \tan\theta_i \left| \int_0^L d_{33}(Z) \exp\left(\frac{i\pi Z}{l_c \cos\theta_i}\right) dZ \right| \right\}^2 \qquad (2)$$

where $d_{33}(Z)$ is the nonlinear coefficient along poling direction Z, L is the sample thickness, θ_i is internal incident angle, l_c is equal to 24.1818 μm for the IOG-1.

According to the theoretical expression (2), two possible $d_{33}(Z)$ profiles can explain the rapid oscillation superimposed on the slow modulation in Maker fringes results. Schematic diagrams of these profiles are shown in Fig. 6. One has an anodic surface and a bulk layer. The other has only two surface layers on both electrode surfaces. The surface here refers to the length that is less than or comparable to the coherence length of the sample. In order to select the most likely profile for further computer simulation of our experimental results, grinding experiments were carried out on our poled samples. For these experiments samples were poled at the same condition as the sample showed in Fig.3. After poling the induced SH Maker fringe pattern was measured. Then one of the two surfaces was polished using an optical fiber polishing paper and after grinding the Maker fringe pattern was measured again. For samples with an induced $\chi^{(2)}$ according to profile A are expected to only show a rapid oscillation after anodic grinding and an unchanged fringe pattern after cathodic grinding. Samples with profile B are expected to only show a slow modulation after either anodic or cathodic grinding. The experimental results, shown in Fig. 7, were in favor of profile A. For profile A, the surface contribution corresponds to the slow modulation and the bulk contribution relates to the rapid oscillation appearing in the fringe pattern.

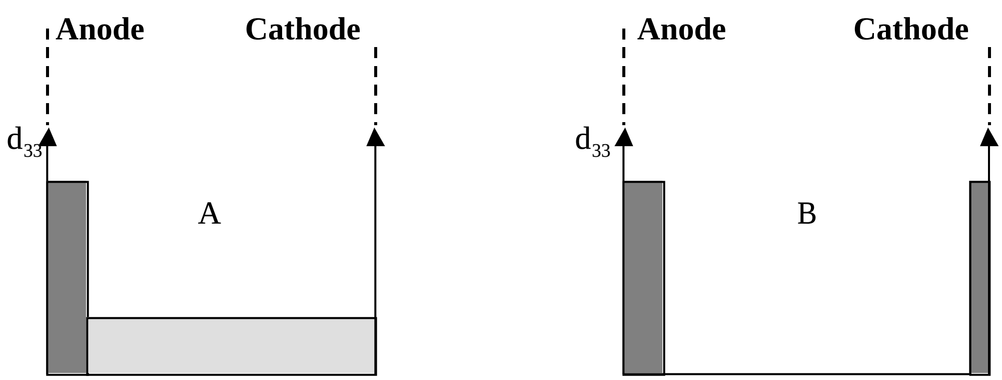

Fig. 6: Two possible $d_{33}(Z)$ profiles

(a)

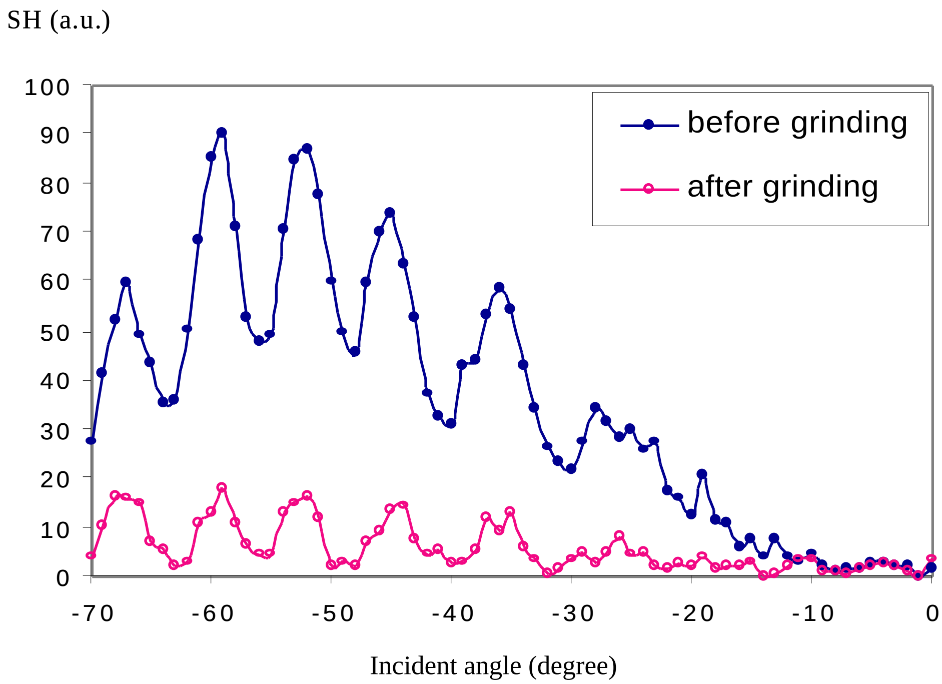

(b)

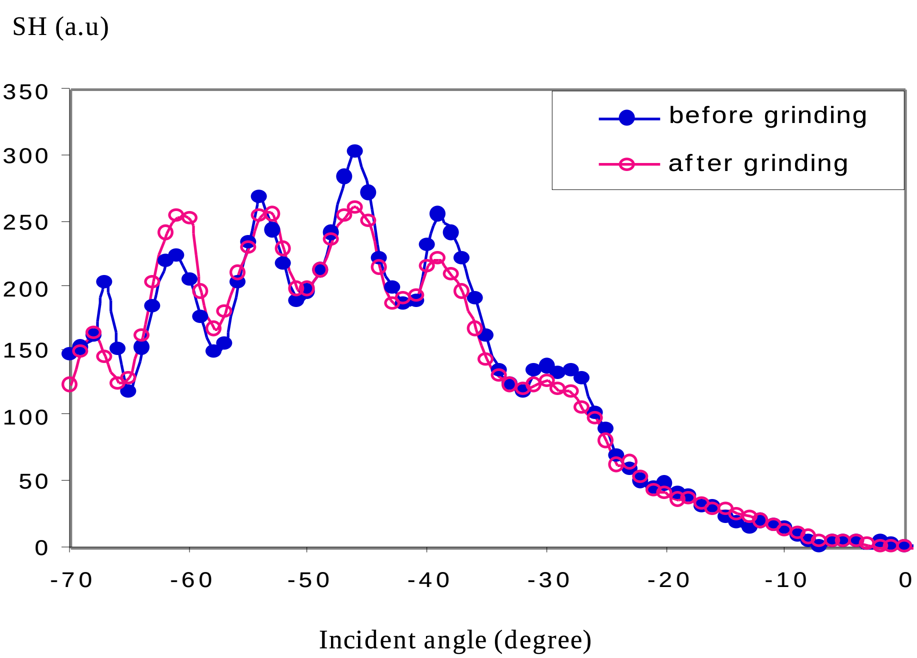

Fig. 7: Grinding experiment on poled samples; (a) anodic surface grinding, (b) cathodic surface grinding.

Based on profile A, the best fit of $d_{33}(Z)$ profile for the result in Fig. 3 is shown in Fig. 8. The computer calculation corresponding to the profile is shown from 0 to 70 degree. The $d_{33, surf}$ (Z) has maximum on anodic surface and decreases linearly with Z for 20 micron thick. The constant $d_{33, bulk}$, which is opposite in sign and at five times magnitude less than the surface coefficient, extends throughout the sample.

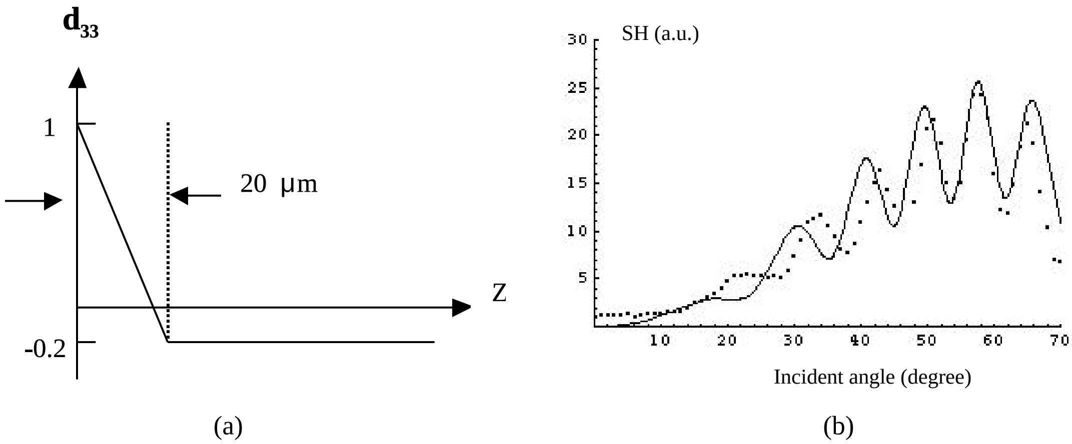

Fig. 8: (a) The $d_{33}(Z)$ profile used in the fit of Maker fringe pattern; (b) Calculated (solid line) and experimental Maker fringe pattern.

From the magnitude of the observed SH signal relative to that of α-quartz we can estimate the nonlinear coefficient to be 0.006 pm/V.

In order to understand how thermal poling leads to the induced $\chi^{(2)}$ profile shown in Fig. 8, it is necessary to develop a model that accounts for the microscopic processes that take place during poling . It has been proposed [16-19] that the surface effect is due to a frozen-in DC field, which is the result of charge separation near the anode in the thermal poling process. This $E_{dc, surf}$ interacts with $\chi^{(3)}$ of the glass, giving rise to the induced $\chi^{(2)}_{surf.}$ However, the origin of the bulk effect is still unclear. It is possible that either there is existence of the induced $E_{dc, bulk}$ due to charge redistribution after the poling process[20-21] or small dipoles/defects are oriented during the process. It can also be combination of both. Our heat treatment experiments after poling show that the surface $\chi^{(2)}$ disappears more rapidly with temperature than the bulk contribution, which could indicate that the surface and bulk nonlinearities have different origins. We are currently carrying out more systematic simulations of our experimental results in terms of the induced $\chi^{(2)}$ profiles. This will yield quantitative information about the surface and bulk nonlinearities as a function of poling voltage, temperature and time. Microscopic models consistent with the observed trends are being developed.

5. CONCLUSIONS

We have induced a $\chi^{(2)}$ in IOG-1 phosphate glasses via thermal poling. The induced nonlinear regions consist of a surface contribution near the anode and a contribution from the bulk. From our theoretical simulation, the surface layer is around 20 micron while the bulk layer extended throughout the sample thickness of 1 mm. Furthermore, the surface d coefficient is larger in magnitude than the bulk coefficient. The contribution of the surface effect as well as the overall SH signals increase as a function of poling voltage, temperature and time.

ACKNOWLEDGMENTS

This work was performed under the auspices of the U.S. Department of Energy by University of California Lawrence Livermore National Laboratory, through the Institute for Laser Science and Applications, under contract No. W-7405-Eng-48. The authors acknowledge financial support from NSF grant ECS 0083087.

REFERENCES

1. T. Findakly , “Glass waveguides by ion exchange: a review”, *Opt. Engineering*, **24**, pp. 244-250, 1985.
2. K. J. Malone, N. A. Sanford, J. S. Hayden, "Integrated optic laser emitting at 906, 1057, and 1358 nm," *Electron. Lett.*, **29**, pp. 691-693, 1993.
3. F. D. Patel *et al.*, “Waveguide fabrication in Nd^{3+} and Yb^{3+} doped phosphate glasses”, OSA TOPS Vol. **19**, *Advanced Solid State Lasers*, Walter R. Bosenberg and Martin M. Fejer (eds.), pp. 446-449, 1998.
4. R. A. Myers *et al*., “Large second order nonlinearity in poled fused silica”, *Opt. Lett.*, **16**, pp. 1732-1734, 1991.
5. V. Nazabal *et al.*, “Second harmonic generation of electrically poled borophosphate glasses: effects of inducing Niobium or Sodium Oxides”, *J. of Solid State Chem*., **133**, pp. 529-535, 1997.

6. F. C. Garcia *et al.*, “Inducing a large second-order optical nonlinearity in soft glasses by poling”, *App. Phys. Lett*., **72**, pp. 3252-3254, 1998.
7. K. Tanaka *et al.*, “Large optical second-order nonlinearity of poled WO_3-TeO_2 glass”, *Opt. Lett*., **25**, pp. 251-235, 2000.
8. P. D. Maker *et al.*, “Effects of dispersion and focusing on the production of optical harmonics”, *Phys. Rev. Lett*., **8**, pp. 21-22, 1962.
9. H. Nasu *et al.*, “Second-harmonic generation from electrically poled SiO_2 glasses: effects of OH concentration, defects, and poling conditions”, *J. Opt. Soc. Am. B*, **12**, pp. 644-649, 1995.
10. Z. Xu *et al*., “Influence of different poling methods on the second order nonlinearity in fused silica glasses”, *Opt. Comm*., **174**, pp. 475-479, 2000.
11. Y. Quiquempois *et al.*, “Localisation of the induced second-order non-linearity within Infrasil and Suprasil thermally poled glasses”, *Opt. Comm.*, **176**, pp. 479-487, 2000.
12. M. Qiu *et al*., “Double fitting of Maker fringes to characterize near-surface and bulk second-order nonlinearities in poled silica”, *App. Phys. Lett*., **76**, pp. 3346-3348, 2000.
13. Z. Xu *et al*., “Nonuniform bulk second-order optical nonlinearity in PbO/B_2O_3 glass”, *App. Phys. Lett*., **77**, pp. 70-72, 2000.
14. J. Jerphagnon and S.K. Kurtz, “Maker fringes: a detailed comparison of theory and experiment for isotropic and uniaxial crystal”, *J. of App. Phys*., **41**, pp.1667-1681, 1970.
15. R. W. Boyd, *Nonlinear Optics*, Academic Press, San Diego, 1992.
16. P. G. Kazansky, P. St. J. Russel, “Thermally poled glass: frozen-in electric field or oriented dipoles?”, *Opt. Comm*., **110**, pp. 611-614, 1994.
17. N. Mukherjee *et al*., “Dynamics of second-harmonic generation in fused silica”, *J. Opt. Soc. Am. B*, **11**, pp. 665-669, 1994.
18. T. Alley *et al.*, “Space charge dynamics in thermally poled fused silica”, J. *of Non. Cryst. Solids*, **242**, pp. 165-176, 1998.
19. A. Le Calvez *et al.*, “A model for second harmonic generation in poled glasses”, *Eur. Phys. J. D*, **1**, pp. 223-226, 1998.
20. A. von Hippel *et al*., “Photocurrent, space-charge buildup, and field emission in alkali halide crystal”, *Phys. Rev.*, **91**, pp. 568-579, 1953.
21. Y. Quiquempois *et al.*, “Thermal poling in silica glasses: evidence of a voltage threshold”, *Technical Digest of BGPP’01*, paper BFA4-1, 2001.